Developmental Biology **218,** 74–88 (2000)
doi:10.1006/dbio.1999.9559, available online at http://www.idealibrary.com on IDEAL®

The Morphology of Heart Development in *Xenopus laevis*

Timothy J. Mohun,[1] Li Ming Leong,[2] Wolfgang J. Weninger,* and Duncan B. Sparrow[2]

*Division of Developmental Biology, National Institute for Medical Research, The Ridgeway, Mill Hill, London NW7 1AA, United Kingdom; and *Department of Anatomy, University of Vienna, Wahringstrasse 13, A-1090 Vienna, Austria*

We have used serial histological sections to document heart formation in *Xenopus laevis*, from the formation of a linear heart tube to the appearance of morphologically distinct atrial and ventricular chambers. 3D reconstruction techniques have been used to derive accurate models from digital images, revealing the morphological changes that accompany heart differentiation. To demonstrate the utility of this approach in analysing cardiac gene expression, we have reexamined the distribution of Hand1 transcripts in the linear and looped heart tube. Our results demonstrate that prior to looping, an initial asymmetric, left-sided pattern is replaced by more symmetrical localisation of transcripts to the ventral portion of the myocardium. After the onset of looping, Hand1 expression is restricted to the ventral ventricular myocardium and extends along the entire length of the single ventricle.

INTRODUCTION

Embryological studies have established that the heart of vertebrates originates from bilateral populations of mesodermal precursor cells formed during gastrulation. In response to signals from underlying endodermal cells, the precardiac mesoderm gives rise to bilaterally symmetrical heart primordia which fuse to form a simple heart tube (Fishman and Chien, 1997). This comprises a muscular myocardial layer that pumps blood through an inner endocardial tube. In the subsequent transition from linear heart tube to multichambered organ, the heart undergoes profound morphological changes, initiated by rightward looping and culminating in chamber formation. Little is known about the molecular mechanisms regulating these events, nor do we yet know the extent to which they are driven by cell lineage or local signalling.

In principle, the amphibian embryo provides an attractive model for studying these events due to its size, its availability, and the ready access it provides to all stages of heart development. Furthermore, in contrast to amniotes, amphibians do not require cardiac function for much of embryonic development. Experimental perturbation of heart formation, including its complete extirpation, has little or no apparent effect on normal embryo development until swimming tadpole stages (Copenhaver, 1926). Despite these advantages, a critical limitation has proved the difficulty in testing the role of individual gene products on heart formation. Ectopic expression of genes can be achieved by direct microinjection of nucleic acids into embryonic blastomeres (for example, Cleaver *et al.*, 1996; Fu *et al.*, 1998; Horb and Thomsen, 1999), but the utility of this technique is restricted by the inability to achieve precise targeting of individual tissues.

An alternative approach is to use transgenesis. In mice, gene knockouts have identified genes required for normal cardiogenesis (Lyons *et al.*, 1995; Lin *et al.*, 1997; Srivastava *et al.*, 1997; Firulli *et al.*, 1998; Riley *et al.*, 1998) and reporter transgenes have been used to identify regulatory regions that confer diverse cardiac-specific patterns of transcription (Kelly *et al.*, 1999). The development of a method for achieving transgenesis in *Xenopus laevis* and its successful adaptation for the diploid relative, *Xenopus tropicalis* (Kroll and Amaya, 1996; Amaya *et al.*, 1998), now raises the possibility that similar approaches can be applied to the study of amphibian cardiogenesis.

A precondition for this is a systematic description of normal heart development in *Xenopus*. This can provide a

[1] To whom correspondence should be addressed. Fax: 0181 906 4477. E-mail: tmohun@nimr.mrc.ac.uk.
[2] These authors contributed equally to this work.

0012-1606/00 $35.00

reference to assess experimentally induced alterations in cardiac morphology and a template for presenting gene expression data. To date, no adequate such description has been published. A series of anatomical studies has detailed the formation of the vascular system in *Xenopus* embryos (Millard, 1945, 1949) but it does not include a description of heart formation itself. A brief, textual account of early cardiogenesis is provided by Nieuwkoop and Faber (1956) as part of a comprehensive outline of *X. laevis* development, but the histological data upon which this was based remain unpublished.

Here, we have attempted to provide an illustrated description of heart formation in *Xenopus*, from the appearance of a linear heart tube to formation of distinct atrial and ventricular chambers. Our data are derived from serial sections of wax-embedded embryos, supplemented with sections from plastic-embedded embryos where greater histological detail was necessary. The results are summarised in accurate 3D models which demonstrate the changing topology of the developing heart tube.

The same methods lend themselves to documenting gene expression patterns in complex structures and we have used them to reassess expression of the putative transcription factor, Hand1, in the *Xenopus* heart. Our results demonstrate that the expression of HAND1 in the myocardium is dynamic. A transitory left asymmetry is established during formation of the linear heart tube, but is rapidly replaced by a symmetrical but ventrally restricted pattern before the onset of looping.

METHODS

Histology

Embryos were staged according to Nieuwkoop and Faber (1956) and fixed in MEMFA (0.1 M Mops, pH 7.4, 2 mM EGTA, 1 mM $MgSO_4$, 3.7% formaldehyde) for 1 h. After dehydration through a graded series of alcohols embryos were embedded in Fibrowax (Difco). Seven-micrometer transverse sections were stained with a Feulgen/light green/Orange G triple stain and images captured using either a Kodak DCS420 digital camera or a JVC KYF55E colour video camera attached to a Zeiss Axiophot microscope. For older embryos, images were also obtained from 4-μm methacrylate sections, stained with haemotoxylin and eosin. Digital images were assembled and filtered using Adobe PhotoShop 5.0 and Extensis Intellihance 3.0 and are available in TIFF or JPEG formats.

3D Methods

For the episcopic method of 3D reconstruction, albino embryos were embedded in Fibrowax, after dehydration in an alcohol series containing lead acetate (Weninger *et al.*, 1998). Tissue was visualised at the surface of the block after successive 7-μm sections using sodium sulphide staining. Sections were cut using a Leica SM2000R sliding microtome and the block was visualised using a JVC TK C1381 video camera attached to a Leica Monozoom7 microscope.

3D models were constructed using the SurfDriver 3.5 software package (www.surfdriver.com). No alignment is necessary for images derived from the episcopic procedure, but images obtained from serial stained sections were aligned according to the notochord before surface rendering (see Results).

Whole-Mount RNA in Situ Hybridisation

Albino embryos were used for whole-mount RNA *in situ* hybridisation as described previously (Sparrow *et al.*, 1998) using probes for XMLC2a (Chambers *et al.*, 1994), XMHCα (Logan and Mohun, 1993), XNkx2-5 (Tonissen *et al.*, 1994), and Hand1 (Sparrow *et al.*, 1998). After being embedded in Fibrowax, serial 10-μm sections were counterstained with Feulgen's reagent and images captured as described above. For 3D reconstruction, no method was available to model the complete range of expression levels evident in sections. Models therefore show precise boundaries for expression domains which may not accurately reflect gradations in transcript levels.

RESULTS

3D Modelling from Serial Section Images

In order to document the morphological steps in *Xenopus* heart formation, we examined serial sections of embryos at successive stages of development, from the onset of myocardial differentiation to the formation of the multichambered tadpole heart. During this 48-h period, the heart primordium undergoes complex morphological changes as a linear heart tube first forms, twists during cardiac looping, and then gives rise to distinct heart chambers. To follow these events we used digital images to derive 3D models of the developing heart.

The derivation of accurate 3D models from serial section data requires independent reference points (fiduciary markers) for alignment of sections and minimal relative distortion between images. Using standard histological procedures, it is difficult to satisfy both these criteria, especially with wax-embedded specimens (Streicher *et al.*, 1997; Weninger *et al.*, 1998). We therefore adopted two approaches to obtain models. First, we used an episcopic method to obtain serial images prior to sectioning (Weninger *et al.*, 1998). In this procedure, image resolution is limited compared with standard staining techniques for wax sections. However, this method overcomes difficulties of section distortion and obviates the need for image alignment. Its accuracy is evident from comparison of 3D models of the stage 35 tadpole with photographs of equivalent-staged specimens (compare Fig. 1A with Figs. 1B and 1C). From these data it is evident that the tadpole notochord forms a reasonably linear rod along the length of the tadpole, including over the developing heart. It can therefore provide a reference AP axis for 3D models.

We also took advantage of this observation to obtain a second series of models by using the centre of the notochord as reference point for aligning images from stained, serial wax sections. Such colour images provided much greater histological detail than the monochrome images from the episcopic procedure but can be severely distorted during the sectioning and staining. Fortunately, the impact of this on

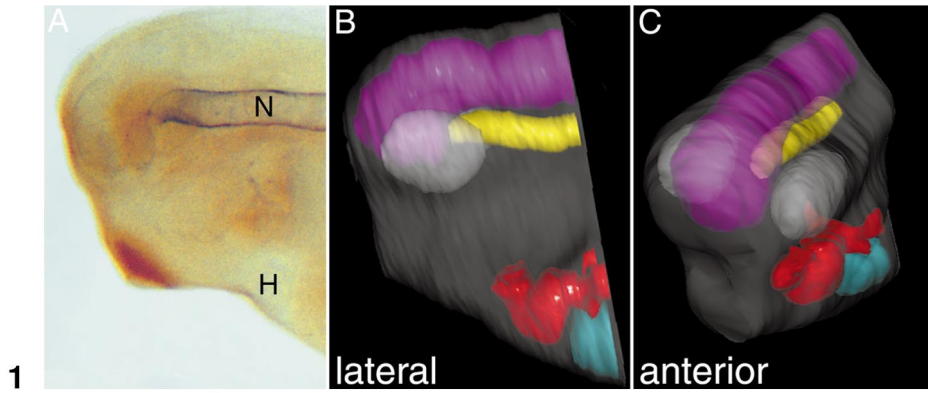

1

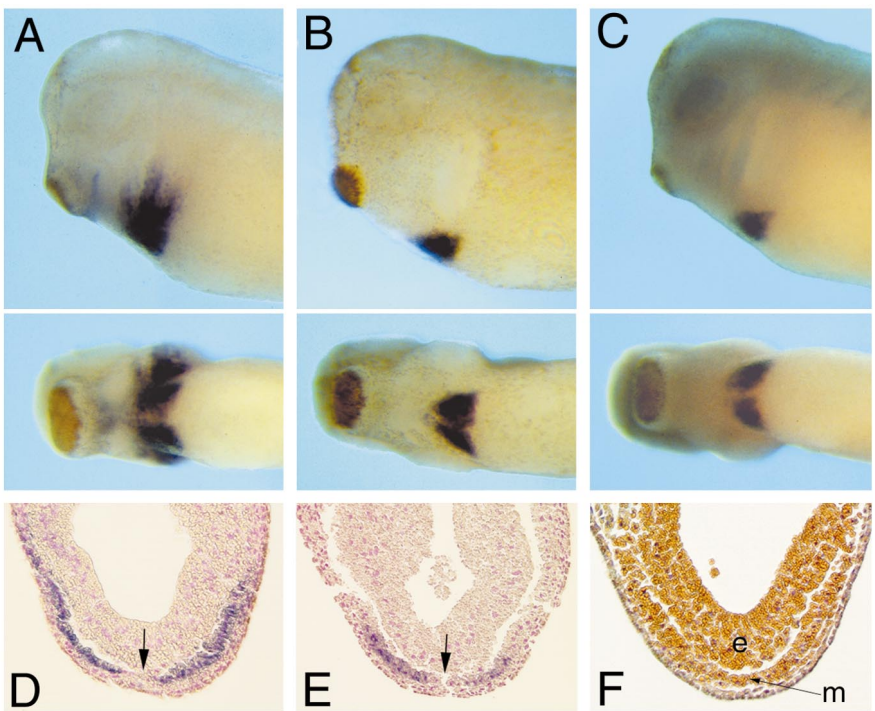

2

FIG. 1. 3D modelling of the tadpole head region. The notochord provides an appropriate reference structure for 3D reconstruction of the developing heart. (A) Whole-mount immunostaining with MZ15 polyclonal antibody demonstrates that the notochord (N) forms an approximately linear rod above the heart region of the stage 34 tadpole. Episcopic images from a stage 35 embryo yield 3D models (B and C) which accurately reproduce organ morphology. Brain (magenta), notochord (yellow), eyes (white), heart tube (red), liver primordium (cyan). Note the spiral shape of the looping heart tube and its extension (as the sinus venosus) over the dorsal surface of the liver. Posterior bifurcation of the sinus venosus into the Cuverian ducts is also evident.

FIG. 2. Myocardial gene expression precedes overt morphological differentiation. Lateral and ventral views of late tail bud embryos (stage 26/27) after whole-mount *in situ* hybridisation to detect Nkx2-5 (A), XMLC2a (B), and XMHCα (C) gene expression. Transcripts are localised in bilateral domains, clearly separated on the ventral midline. Sections through the heart-forming region show bilateral domains of Nkx2-5 (D) and XMLC2a (E) expression, separated by the ventralmost nonexpressing cells (arrows). Normal, triple-stained sections through the same region (F) demonstrate that the cardiac mesoderm (m) forms a contiguous layer across the ventral midline, clearly distinct from the adjacent endoderm (e).

the 3D reconstruction proved to be minimal after removing the most distorted sections and replacing them with data obtained by interpolation. Overall, no significant difference was found between models obtained with either of the two methods, suggesting that each provided an accurate 3D representation of the developing heart. In both methods, the least successful results were obtained for the endocardial tube, which was particularly prone to distortion after sec-

tioning and was poorly or erratically resolved by the episcopic staining procedure.

Molecular Markers Precede Morphological Differentiation

In all vertebrates, the heart is formed from mesodermal progenitors which appear bilaterally and subsequently fuse into a single domain. In *Xenopus*, cardiac mesoderm arises below the anterolateral edges of the neural plate, on either side of the embryo. This tissue moves ventrally and merges on the ventral midline to form a single heart field (Sater and Jacobson, 1990). These events can be visualised using the *Xenopus* tinman homologues, Nkx2-5 (Tonissen *et al.*, 1994) and Nkx2-3 (Evans *et al.*, 1995), which are expressed initially in the bilateral regions of cardiac mesoderm and form a single anteroventral domain of expression behind the cement gland of the late neurula embryo. This region encompasses the myocardial progenitors, but it is formed many hours before the onset of cardiac muscle differentiation and extends much further into both anterior and dorsolateral mesoderm (Tonissen *et al.*, 1994; Evans *et al.*, 1995) as well as the adjacent pharyngeal endoderm.

In later tail bud stages, the single Nkx2-5/Nkx2-3 expression domain separates briefly once more, forming distinct patches of expression on either side of the ventral midline (Fig. 2A), which rapidly fuse once more into a single domain. This transitory reappearance of bilateral Nkx2-5 expression coincides with the onset of cardiac muscle differentiation, as detected by the appearance of transcripts encoding the cardiac muscle-specific proteins MHCα, MLC2a, and troponin Ic (Logan and Mohun, 1993; Chambers *et al.*, 1994; Drysdale *et al.*, 1994). Like the tinman homologues, these are first detected in a bilateral pair of triangular domains separated by the ventral midline, posterior to the cement gland of the late tail bud embryo (stages 26/27) (Figs. 2B and 2C).

The apparent reappearance of bilateral cardiac mesoderm domains is not due to the loss of ventral mesodermal tissue, since transverse sections through the heart-forming region at this stage demonstrate that the mesodermal layer remains continuous across the ventral midline, despite the bilateral appearance of MLC2a and MHCα expression (compare Figs. 2D and 2E with 2F). Rather, these data suggest that mesodermal cells on the ventral midline either cease expressing tinman homologues or originate outside of the Nkx2-5-expressing domain and migrate to their ventral position. No lineage- or fate-mapping data are available to resolve these alternatives or to identify the subsequent role of these cells in older embryos. Intriguingly, the same ventralmost mesodermal cells can be distinguished from more lateral cells not only by the absence of myocardial markers, but also by the expression of the Hand1 gene (Sparrow *et al.*, 1998), which is subsequently expressed in both the myocardium and the great vessels.

After the onset of myocardial differentiation, expression of both the tinman homologues and the myocardial markers rapidly extends once more across the ventral midline. As a result, differentiating myocardial tissue forms a single wedge-shaped domain, oriented along the AP axis and encompassed by a single broader domain of Nkx2-5 and Nxk2-3 expression. It is unclear whether this results from reactivation of the tinman homologues in the ventralmost mesoderm, resulting in the delayed onset of differentiation, or the migration of these cells elsewhere in the embryo.

Formation of a Myocardial "Trough"

Within a few hours, extensive changes have occurred in the morphology of the cardiac mesoderm. Transverse sections from embryos at stage 29/30 show that the anterior ventral mesoderm now comprises splanchnic and somatopleural layers. Each is a single cell thick, but the splanchnic layer is considerably thickened throughout the heart-forming region. At its anterior end, the splanchnic layer is no longer tightly apposed to the endoderm, and endothelial cells of the newly formed endocardial tube can be seen in the gap between endoderm and mesoderm (Fig. 3, section 5). In successive sections, the splanchnic layer forms a progressively more pronounced ventral trough of myocardial tissue encompassing the endocardial tube. The somatic mesoderm remains as a thin, single-cell layer apposed to the ventral ectoderm, forming the ventral and lateral walls of the pericardial cavity (Fig. 3, sections 11–17).

3D reconstruction of the heart primordium at this stage (Fig. 3) demonstrates that the endocardial tube is not linear, rather it bends ventrally from anterior (future outflow tract) to posterior (future sinus venosus). The myocardial trough encloses the endocardial tissue more completely in posterior sections, with the result that two distinct regions of the cardiac mesoderm can be distinguished: the ventrolateral walls of the trough and the dorsolateral wings of mesoderm. The former gives rise to the myocardium whilst the latter become the dorsal mesocardium and pericardial roof (Raffin *et al.*, 1999).

Linear Heart Tube Stages

By stage 32, much of the myocardial trough has closed over the dorsal surface of the endocardial tissue to form a linear heart tube (Fig. 4). As a result, mesoderm initially adjacent to and contiguous with the myocardial tissue on either side of the embryo is brought together to form the dorsal mesocardium and the pericardial roof. However, at its anterior end, the myocardial layer retains an open structure and the endocardial tube broadens into a wide sinus (the aortic sac) that extends forward into the ventral aorta and bilaterally into the first aortic arch.

At its posterior end, the endocardial tube forms the sinus venosus which bifurcates and extends caudally over the dorsal surface of the liver primordium. Myocardial tissue encloses the dorsal and lateral surfaces of the sinus venosus extending approximately to the point of bifurcation. Caudal to this, the splanchnic mesoderm layer remains contiguous

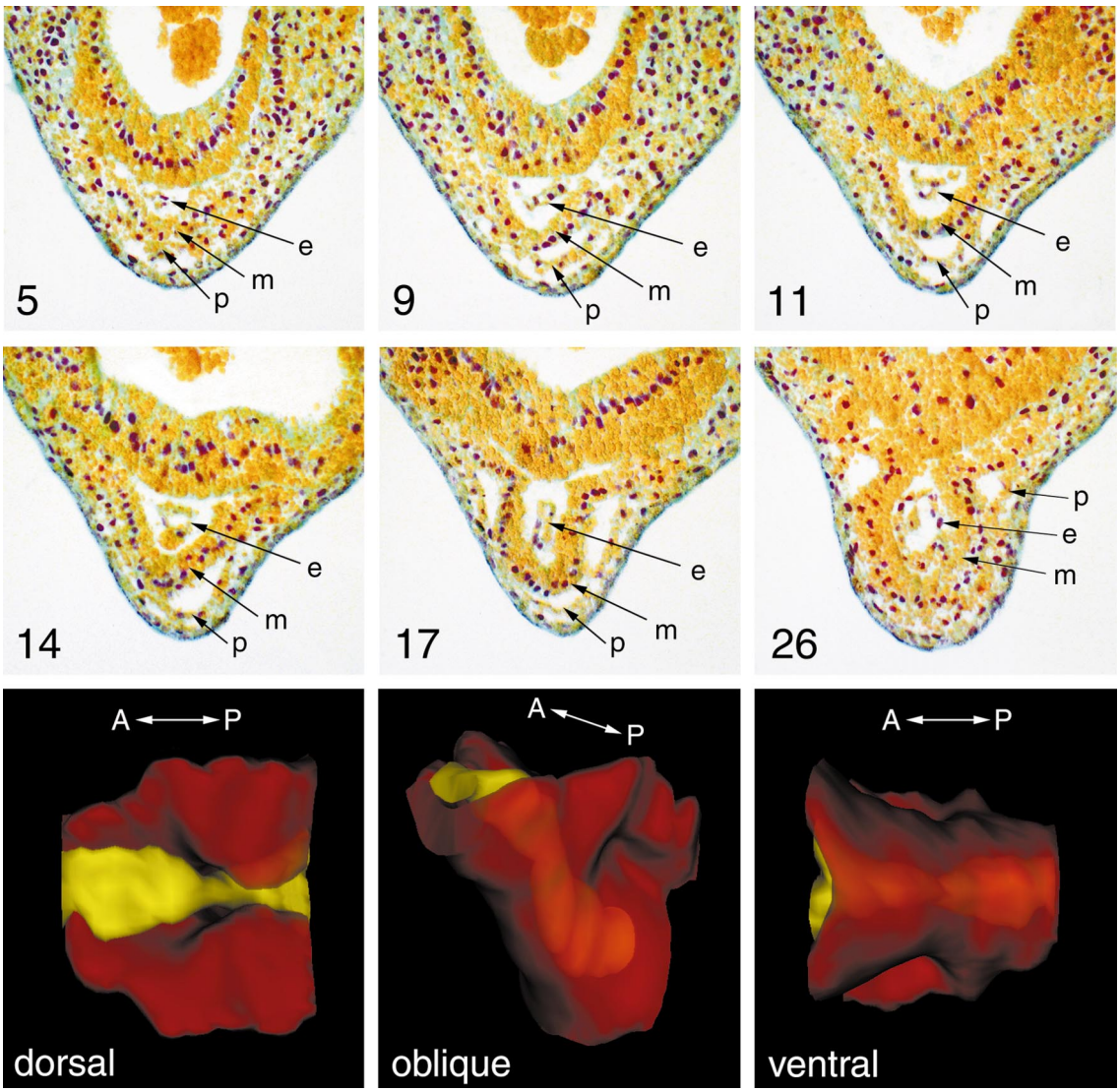

FIG. 3. Formation of the linear heart tube (stage 29). Transverse sections through the anteroventral, heart-forming region, showing endocardial (e), myocardial (m), and pericardial (p) cell layers. Sections (7 μm) are numbered commencing from the anterior end of the pericardial cavity. 3D models (viewed as indicated) demonstrate that the thickened, myocardial region of the splanchnic mesoderm (red) forms a trough, within which lies the endocardial tube (yellow).

but does not express myocardial differentiation markers (data not shown).

The linear heart tube structure is maintained for several hours (stage 33) during which time the dorsal mesocardium becomes more elongated, especially in the posterior half of the heart, and the major vessels of the venous system are formed (Millard, 1949). The two horns of the sinus venosus form the common cardinal sinuses (Cuverian ducts), which traverse the lateral sides of the anterior gut endoderm, ascending to join the posterior cardinal veins via the pronephric sinus. On the ventral sides of the gut endoderm, the newly formed omphalomesenteric (vitelline) veins enter the sinus venosus immediately posterior to its bifurcation.

Heart Tube Looping

By stage 35 (Fig. 5), the posterior region of the heart tube (presumptive atrium and sinus venosus) lies dorsal relative to the more anterior, ventricular region and the entire heart tube is no longer linear along the AP axis, rather it has formed an anticlockwise spiral. Hence, in anterior to posterior sequence, the anterior portion of the outflow tract (truncus arteriosus) lies medially; the posterior portion

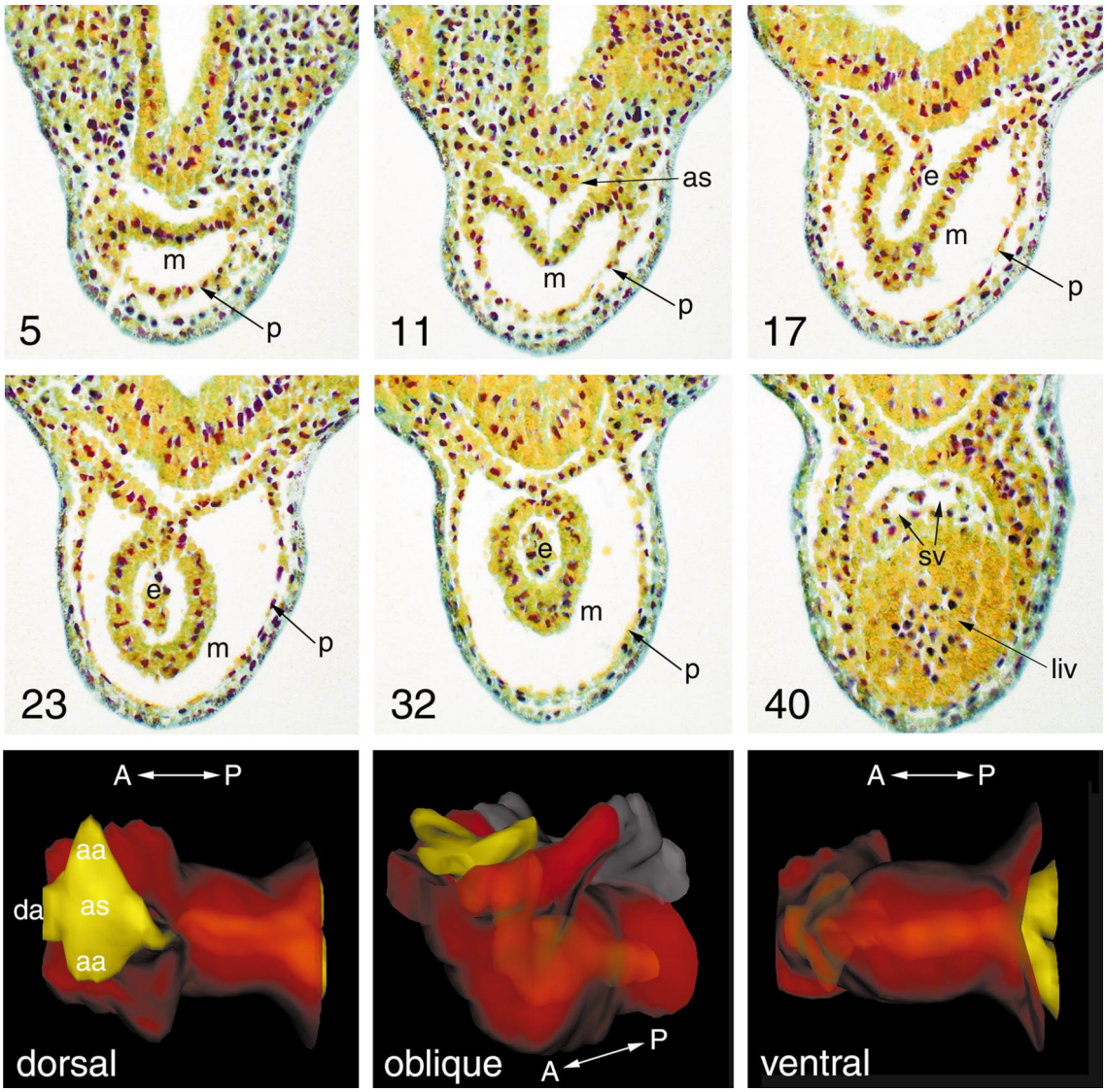

FIG. 4. Completion of a linear heart tube (stage 32). Transverse sections demonstrate that by this stage, the myocardium has formed a complete tube surrounding the endocardium in all but the most anterior region (see Fig. 3 legend for labelling details). The most posterior sections show bifurcation of the endocardial tube into the sinus venosa (sv), dorsal to the liver primordium (liv). 3D models (dorsal view) show the aortic sac (as) at the anterior end of the endocardial tube, as well as the ventral aorta and first aortic arch (aa). (For clarity, the dorsal mesocardium and pericardial roof (grey) are omitted from dorsal and ventral views.)

(conus) is increasingly displaced to the right side of the embryo as it descends into the pericardial cavity. Central sections show the ventricular region lying first on the right and then on the left side of the embryo, whilst the atrial region and sinus venosus are medially positioned (Figs. 5 and 8A–8C). *In situ* hybridisation data indicate that myocardial tissue continues to cover the dorsolateral aspect of the endocardium, anterior to its bifurcation in the sinus venosus. The ventral surface of the sinus venosus lies in contact with the developing liver (Fig. 5, section 34 and 3D model, ventral view), which occludes the ventral half of the pericardial cavity. At its anterior end, the endocardial tube ascends almost vertically through the outflow tract, turning 90° before extending in an anterior direction into the ventral aorta and flanking branches of the first aortic arch.

Despite these morphological changes, there is little else evident from histological sections that distinguishes future chambers of the heart. Outflow tract and ventricular and atrial regions of the myocardium are all similarly thickened at this stage (Figs. 8A–8C), as is the dorsal pericardium that underlies the aortic sac. Furthermore, none of the characteristic constrictions that demarcate future chambers of

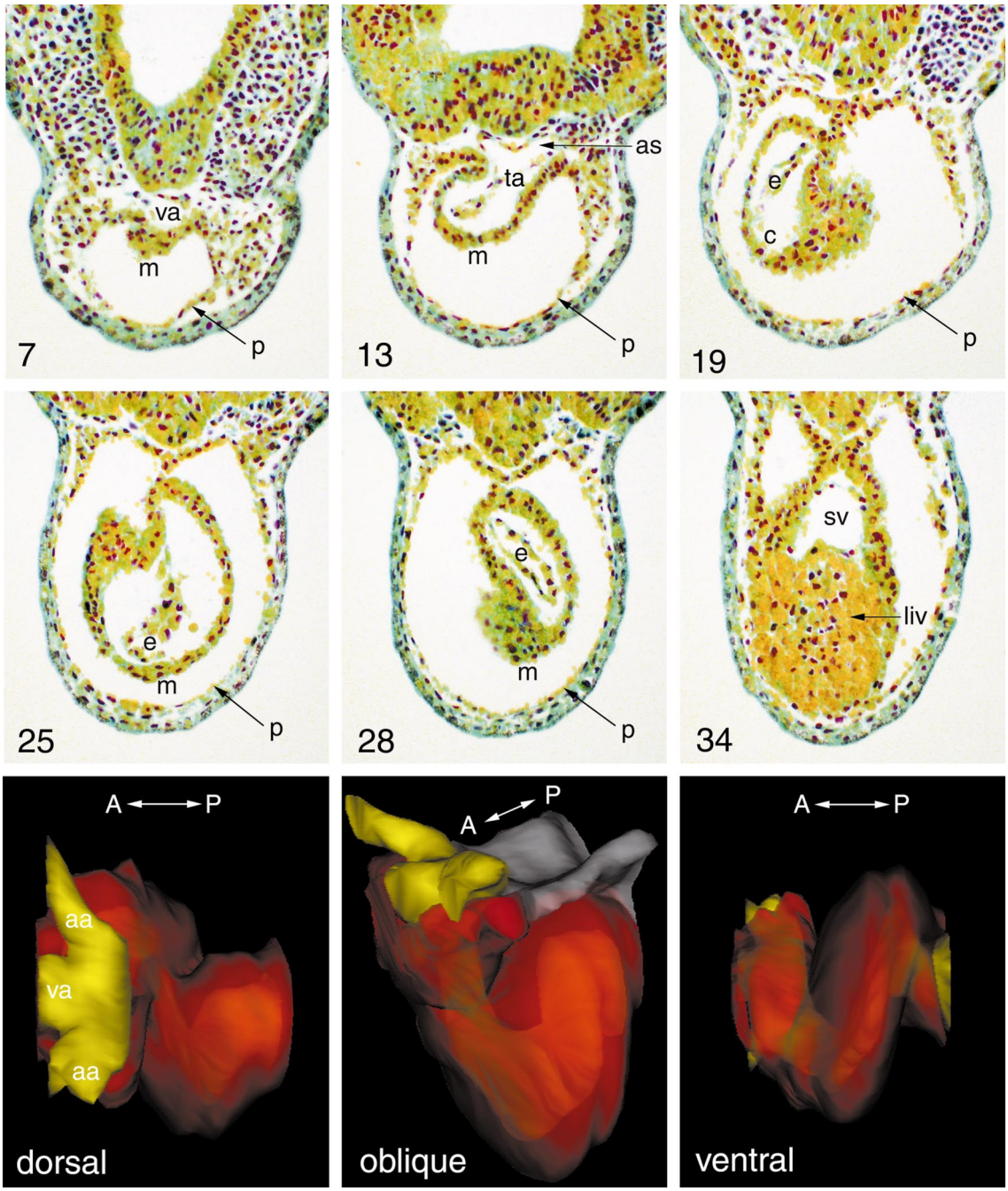

FIG. 5. Spiral looping of the heart tube (stage 35). Transverse sections through the looped heart tube show the medial location of the truncus arteriosus (ta) and rightward displacement of the adjacent conus region (c) (see Figs. 3 and 4 for further labelling details). 3D models reveal the anticlockwise spiral formed by the looping heart tube. (For clarity, the dorsal mesocardium and pericardial roof (grey) are omitted from dorsal and ventral views).

mammalian and avian embryos (the atrioventricular and interventricular sulci) are evident in 3D models of the *Xenopus* heart tube (Fig. 6).

From nuclei counts, it is possible to investigate whether the morphological changes of heart tube closure and looping are accompanied by major changes in cell number. Table 1 compares the number of nuclei evident in successive pairs of sections from the heart tube between stages 32,

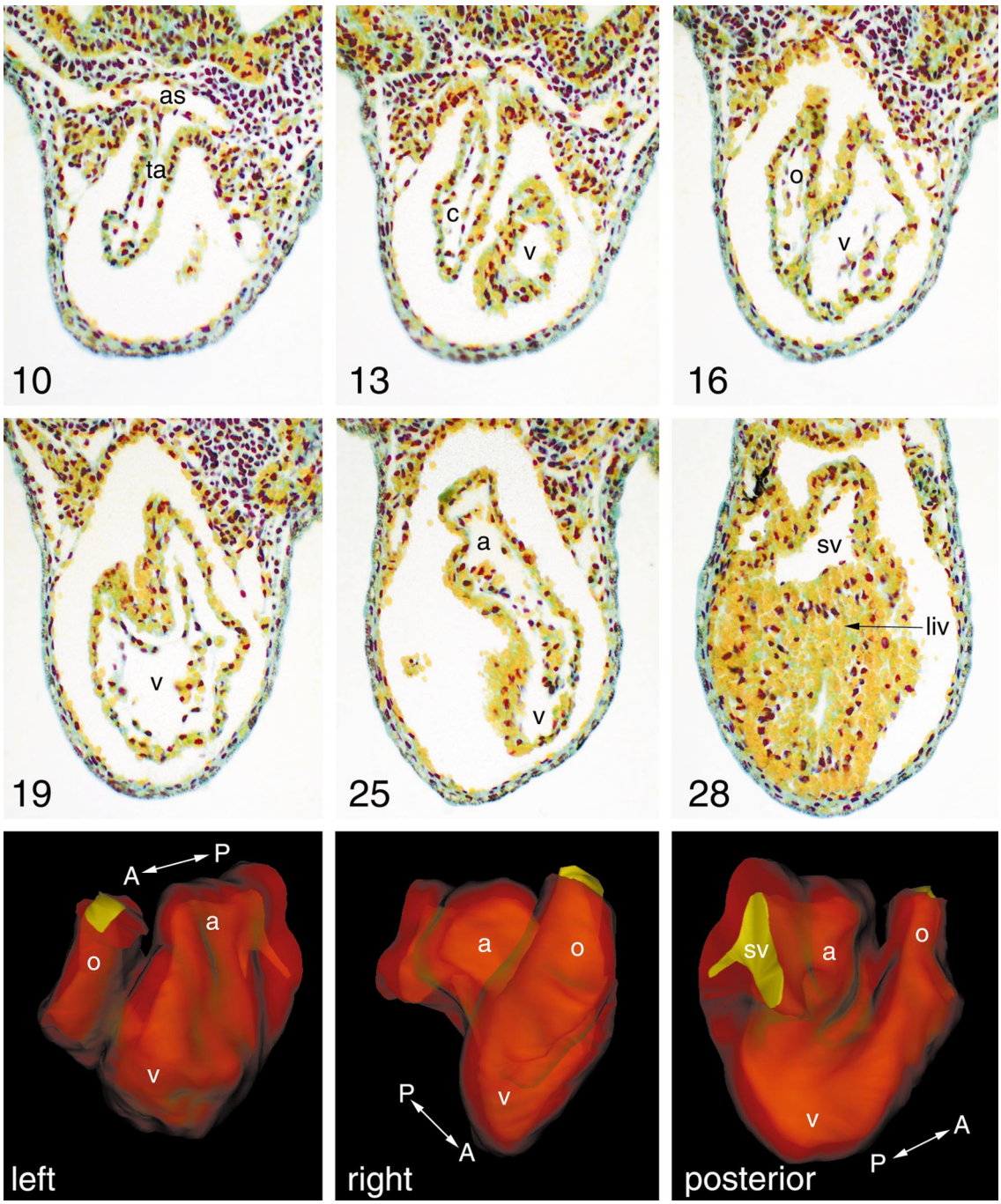

FIG. 6. The onset of chamber formation (stage 40). Transverse sections indicate the complexity of heart morphology by this stage. Anterior and posterior regions of the outflow tract (truncus arteriosus and conus, respectively) can be identified; ventricular (v) and atrial (a) regions have formed in an anterior to posterior sequence along the looped tube. Some thickening of the ventricular myocardium is evident, but is more clearly resolved in plastic sections (see Fig. 7). 3D models of the inner (yellow) and outer (red) surfaces of the myocardium demonstrate that the atrial region lies both dorsal and posterior to the ventricle. A broad sinus (sv) extends from the atrial region over the developing liver before bifurcating into the Cuverian ducts.

TABLE 1

Section pair[a,b]	St32 Total	St32 Myo[c] (%)	St33/34 Total	St33/34 Myo[c] (%)	St35 Total	St35 Myo[c] (%)
1	16.5	—	11	—	23.5	—
2	21.5	8 (37)	17.5	—	42.5	16.5 (39)
3	24	16.5 (69)	29.5	22 (75)	45	35.5 (79)
4	36.5	28 (77)	30.5	23 (75)	44.5	33.5 (75)
5	43	31.5 (73)	31	24 (77)	48	38 (79)
6	48.5	36 (74)	45.5	31.5 (69)	62.5	50 (80)
7	50	36 (72)	48	31 (65)	78.5	59.5 (76)
8	49.5	33.5 (68)	49.5	30 (61)	77.5	66 (85)
9	50.5	34.5 (68)	46	34 (74)	78.5	66.5 (85)
10	45.5	29.5 (65)	53	35.5 (67)	81	69.5 (86)
11	48	32 (67)	57	42 (74)	64.5	52.5 (81)
12	47.5	32 (67)	55.5	41 (74)	55	42.5 (77)
13	49	34 (69)	50.5	35.5 (70)	32	20 (63)
14	40.5	28.5 (70)	45	31 (69)	33	9.5 (29)
15	41	27 (66)	35.5	21.5 (61)	—	—

[a] Values shown were obtained by first counting Feulgen-stained nuclei in the heart tube (myocardium, mesocardium, and dorsal pericardium) in individual 7-μm sections. The values shown represent an average value for successive pairs of sections within each series.

[b] Section pairs are numbered according to their relative location along the AP axis but do not provide absolute reference positions for comparison between embryo stages.

[c] In all but the most anterior sections, it was possible to estimate whether nuclei lay within myocardial tissue (rather than dorsal pericardium and mesocardium) using a combination of morphological criteria (see Results) and *in situ* hybridisation data for myocardial markers carried out with similar-staged embryos.

33/34, and 35. At the earliest of these stages, all but the most anterior regions of the linear heart tube comprise 40–50 cells in cross section, 70–75% of which are myocardial. Little change in either cell number or proportions is evident at stage 33/34, but looping is accompanied by an approximate doubling in cell number within the central (looped) portion of the myocardium, with smaller increases at anterior and posterior portions of the heart tube. In contrast, the number of cells comprising dorsal mesocardium and the adjacent pericardial roof remains approximately constant over the same stages.

Chamber Formation

In the next 16 h, both the heart tube and the pericardial cavity become more extended along the dorsoventral axis. The spiral looping of the tube becomes compressed along the AP axis with the result that by stage 39/40, the atrial region lies almost directly dorsal to the ventricular tissue (Fig. 6). Profound differences are now evident in the myocardium along the length of the tube (Figs. 8D–8F). In the atrial region, the wall is little thicker than the endocardium itself, whilst in the more ventrally located ventricular region and in the outflow tract, the myocardium is many times thicker. Subsequently, the ventricular myocardial wall becomes thicker still (Figs. 7 and 8G–8I) with the formation of trabeculae, which are largely confined to the outer curvature of the ventrolateral wall.

Valve formation occurs over the same period (Nieuwkoop and Faber, 1957) and by stage 45/46, both the spiral valve within the outflow tract and the atrioventricular valve can clearly be resolved (Fig. 7, sections 12 and 19). The last major step in tadpole heart formation is atrial septation. In Fig. 7, an atrial septum can be seen extending from the dorsal wall of the atrium most of the way towards the atrioventricular aperture, incompletely separating the two atrial chambers (sections 19 and 36). This division is unequal, the right atrium being noticeably larger than the left. Caudally, the septation is complete, the left and right atrial chambers being contiguous with the pulmonary vein and sinus venosus, respectively. Interestingly, a third vessel lumen can be detected ventral to the pulmonary vein in some embryos (for example Fig. 7, section 40, arrowhead) but is present only in a few sections immediately caudal to the atria. 3D models reveal that this represents a connection between the sinus venosus and the left atrium (Fig. 7, 3D model, left and oblique views), which is lost in slightly older tadpoles.

Regionalised Expression of Hand1 (eHand)

3D modelling techniques are a powerful aid in analysing the changing morphology of the developing heart and they may also help in clarifying the spatial patterns of gene expression associated with these changes. To test this possibility, we have examined the expression of Hand1

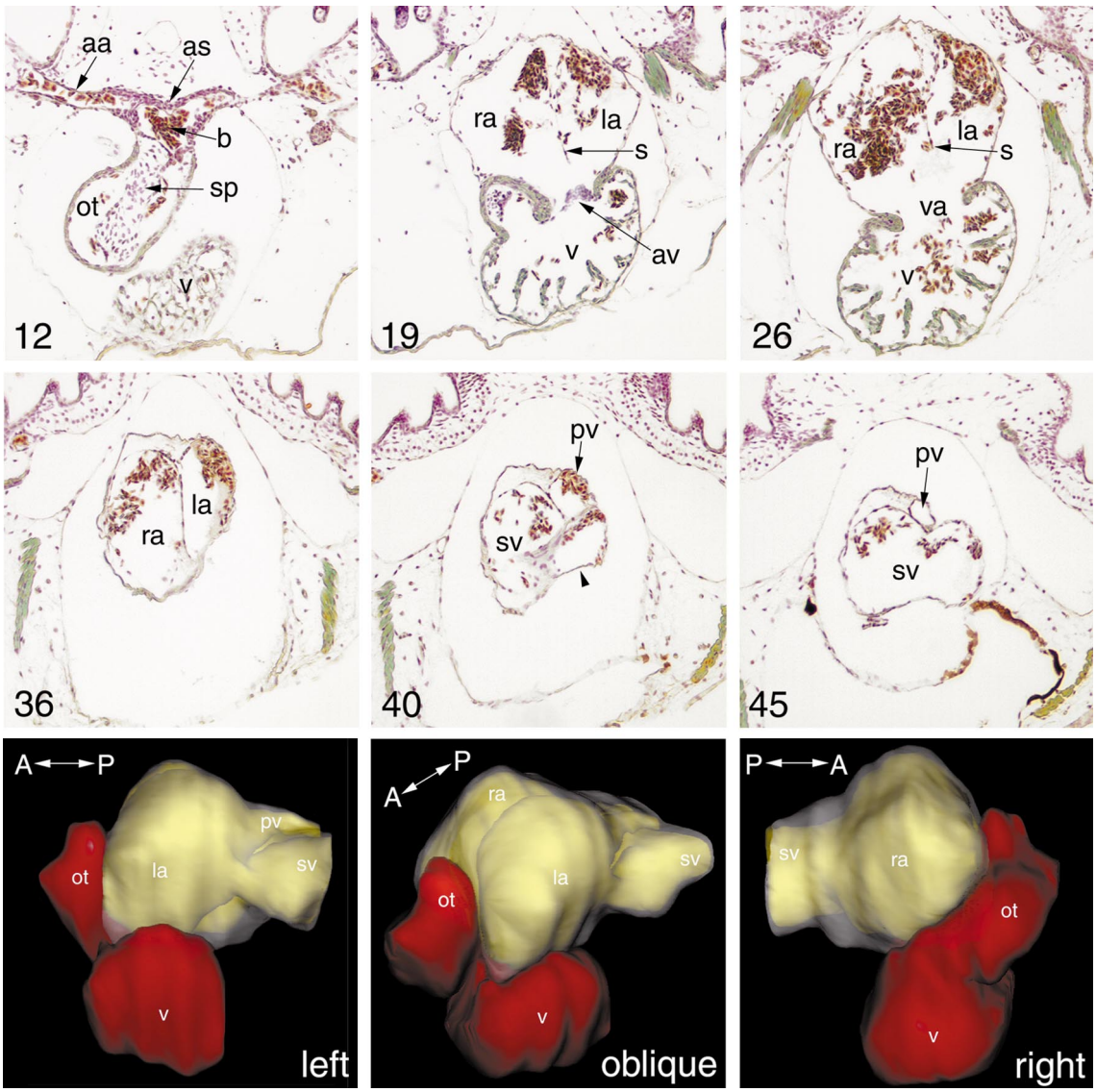

FIG. 7. Completion of the three-chambered heart (stage 46). Transverse sections are numbered in cranial–caudal sequence, beginning with the most anterior portion of the outflow tract. Blood cells (b) are present throughout the heart chambers and are particularly prominent in the aortic arch (aa), aortic sac (as), and atrial chambers. The spiral valve (sp) can be seen partitioning blood flow from the outflow tract (ot) to the aortic sac. The ventricular myocardium shows extensive trabeculation and local thickening at the atrioventricular aperture (va). The atrioventricular valve (av) separates atrial and ventricular chambers. Dorsal to the ventricle (v), a septum (s) incompletely divides the thin-walled atrial chamber into left (la) and right (ra) atria. In more caudal sections, septation is complete. 3D models reveal the separation of inflow from the sinus venosus (sv) and pulmonary vein (pv), which supply the right and left atria, respectively. At the stage shown, a small connection between the left atrium and the sinus venosus can also be seen (section 40, arrowhead; 3D model, left view). This is lost in older embryos.

(eHand) in the linear and looped heart tube. The vertebrate HAND genes encode bHLH proteins and are expressed in a wide variety of tissues during early development, including both myocardial and pericardial tissue (Srivastava *et al.*, 1995). Their expression is best characterised in the mouse, in which the Hand genes are expressed in complex and distinct patterns within the developing heart. After cardiac looping, Hand1 (eHand) is expressed in the outer curvature of the future left ventricle whilst Hand2 (dHand) is expressed throughout the myocardium, becoming more prominent in the outer curvature of the prospective right ventricle. These patterns are maintained even when the sidedness of the heart is reversed, as in the inv mutant mouse which exhibits situs inversus (Thomas *et al.*, 1998).

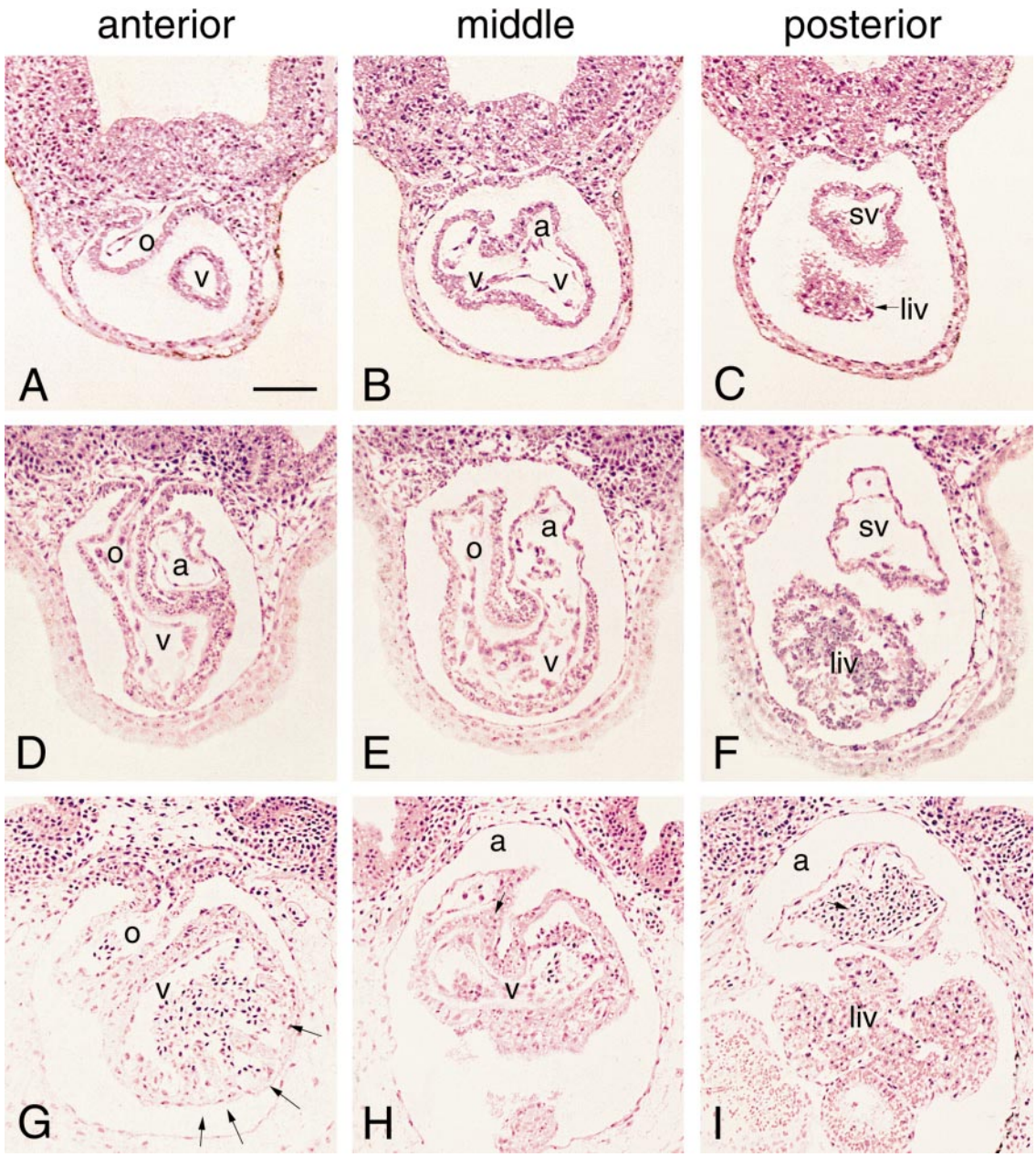

FIG. 8. The acquisition of distinct chamber morphologies is clearly resolved in transverse sections from methacrylate-embedded embryos. (A–C, D–F, and G–I) Sections through the anterior, middle, and posterior regions of the heart tube at stages 35, 39, and 42, respectively. At the onset of looping (stage35), the myocardial walls of the outflow tract (o), ventricular (v), atrial (a), and posterior sinus (sv) regions are of equal thickness. By stage 39, differential thickening is evident in the outflow tract and ventricular region. At stage 42, trabeculae (arrows) have formed in the lateroventral wall of the ventricular myocardium. (Blood cells are evident throughout the heart at this stage.) Bar represents 100 μm.

Furthermore, Hand2-null mice fail to form a right ventricle (Srivastava *et al.*, 1997). These findings have led to the suggestion that the Hand genes might play a role in establishing distinct identities for systemic and pulmonary ventricles (Thomas *et al.*, 1998).

At earlier stages of mouse cardiogenesis, the precise distribution of the Hand1 transcripts is controversial. Biben and Harvey (1997) demonstrated that the caudal domain of Hand1 initially comprised both ventricular and atrial regions of the linear heart tube, as well as the sinus venosa. In

contrast to the predominantly left-sided pattern of expression in the looped heart tube, early expression is symmetrical about the L/R axis. Strikingly, they found that Hand1 transcripts were restricted to the ventral wall of the myocardium, an observation subsequently confirmed by Thomas *et al.* (1998) and providing evidence for the early establishment of dorsoventral asymmetry in the linear heart tube. The earlier study (but not the later one) also found a second phase of expression during which transcripts were detected in an asymmetric, left-sided pattern prior to the onset of looping. In embryos lacking the homeobox transcription factor Nkx2-5, the heart tube fails to loop and lacks left-sided Hand1 expression (Biben and Harvey, 1997). Together, these findings led to the suggestion that an early role for the Hand1 gene lies in mediating signals that establish cardiac laterality (Biben and Harvey, 1997). Gene-targeting experiments support this proposal. Targeted disruption of the Hand1 gene results in early lethality, due to extraembryonic defects (Firulli *et al.*, 1998; Riley *et al.*, 1998) but tetraploid-rescued Hand1-null mouse embryos arrest later in development (E10) with unlooped heart tubes (Riley *et al.*, 1998).

The disputed nature of the Hand1 expression pattern in the mouse embryo has led us to examine expression of the *Xenopus* gene, and in an earlier study we found a predominantly left-sided domain of expression at the linear heart tube stage (Sparrow *et al.*, 1998). We have now applied the 3D reconstruction methods described above to provide a detailed model of Hand1 expression throughout the heart tube, before and after the onset of looping.

Prior to looping (Fig. 9A), Hand1 expression appears widespread throughout the pericardium. Expression also extends throughout the anterior myocardial sheet (section 3). In more posterior sections, staining is reduced to background levels in the right wall of the myocardial "trough" but maintained in the adjacent prospective pericardial roof (section 7). In subsequent sections, a gap in staining emerges at the junction of the left myocardial wall and the pericardial roof (section 9) and the domain of staining shifts progressively towards the ventral side of the myocardium (section 17). 3D models of such data confirm this transition from initially symmetrical and uniform expression throughout the myocardium, first to a left-sided and then to a more ventrally restricted domain. In contrast, Hand1 expression is maintained in both left and right sides of the dorsal pericardium along the length of the heart tube.

After the onset of looping (Fig. 9B), Hand1 expression remains restricted primarily to the ventral and left ventrolateral portions of the myocardium in the central region of the heart tube (sections 13 and 22). This tissue corresponds to ventricular myocardium and subsequently forms the single ventricle. Staining is uniform and heavy throughout the outflow tract but is absent from the posterior atrial region and the sinus venosus (sections 22 and 24 and 3D models). Within the pericardium, levels of Hand1 transcripts are maintained in the pericardial roof but are sharply reduced in the lateral and ventral regions.

DISCUSSION

Amphibian Heart Formation

Much of our knowledge about amphibian cardiogenesis derives from the work of classical embryologists, who analysed the origins of heart tissue and the tissue interactions necessary for heart development. Their work provided a detailed description of heart formation in the urodele amphibian, *Ambystoma* (Mohun and Leong, 1998, and references therein). No comparable, pictorial account of heart formation is available for the anuran, *Xenopus*, which is now the predominant amphibian used for developmental and molecular studies. The current work is an attempt to provide at least part of such an account. Initially, we have restricted our study to the formation, looping, and compartmentalisation of the linear heart tube (stages 28–42), events which lend themselves to simple histological and 3D reconstruction techniques. Later events of valve formation and chamber septation require the resolution provided by serial plastic sections and alternative methods of 3D reconstruction, such as the EMACS procedure (Streicher *et al.*, 1997) or confocal microscopy (Kolker *et al.*, 1999).

Overall, our data are consistent with earlier accounts (Nieuwkoop and Faber, 1956), but also emphasise four features which characterise *Xenopus* cardiogenesis. First, heart tube formation begins with the formation of a single endocardial tube along the ventral midline, between the endoderm and the splanchnic layer of mesoderm. This contrasts with the fusion of bilaterally formed endocardial tubes described for amniotes. Second, the formation of a linear heart tube occurs progressively along the AP axis, being most advanced in the posterior region. As a consequence, closure of the heart tube and formation of the dorsal mesocardium first occur at the caudal end, extending cranially as development proceeds. Third, looping produces a heart tube that has been described as S-shaped but is perhaps more accurately considered spiral. This results in a convergence between the right–left and dorsoventral axes (see below). Fourth, after looping, the endocardial tube extends a considerable distance over the liver primordium as a single sinus (sinus venosus) before bifurcation into bilateral horns (compare Figs. 4 and 6).

Hand1 Expression

3D reconstruction has particular value in the study of structures with complex or dynamic morphology such as the developing vertebrate heart. Here we have used this approach to investigate expression of the putative transcription factor, Hand1. Our models demonstrate that at the linear heart tube stage, the pattern of expression varies dramatically along the AP axis. Uniform expression throughout the anterior myocardial plate is replaced by left-sided expression in the forming tube (or myocardial trough) and this in turn is followed by symmetrical, ventral expression in the myocardium of the posterior region. Since development of the heart tube at this stage is progressively

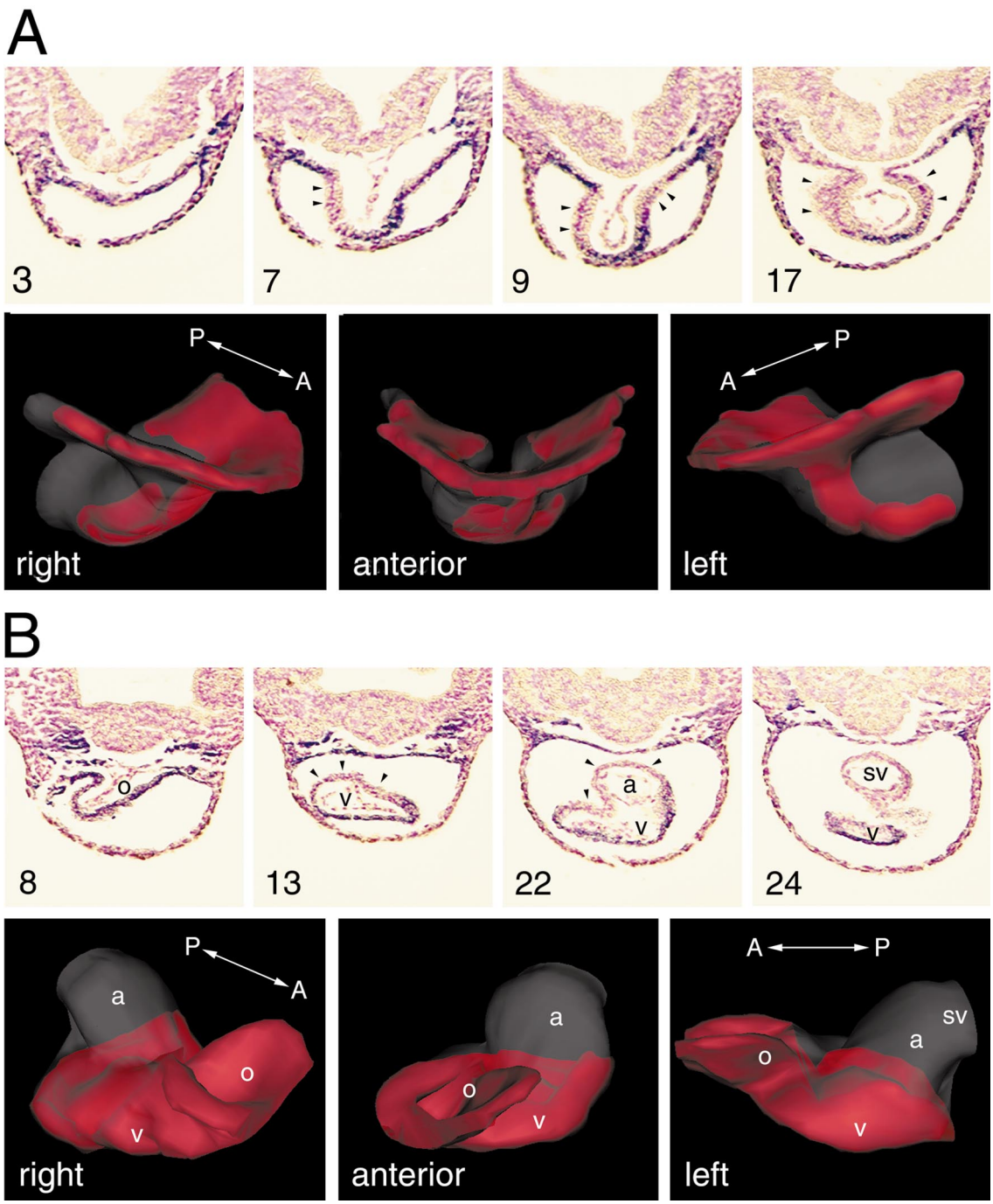

FIG. 9. Expression of *Xenopus* Hand1 in the heart tube. Hand1 transcripts were visualised by whole-mount RNA *in situ* hybridisation (purple) in embryos at the linear (stage 30) and looped (stage 35) heart tube stages (A and B, respectively). Serial 10-μm transverse sections were numbered from the beginning of the pericardial cavity and representative examples are shown. At the linear tube stage, staining is absent from the left myocardial wall (arrowheads) in anterior sections and increasingly from the right myocardial wall in more posterior sections. In the looped heart, little or no staining is detected in the dorsal wall of the ventricle or the atrial myocardium (arrowheads). 3D models constructed from these data show the Hand1 expression domain (red) superimposed on a model of the myocardium (opaque). (Note that some distortion has occurred as a result of the whole-mount procedure, resulting in compression of the heart loop in both AP and DV axes.)

more advanced along the AP axis, these results may well represent the developmental sequence of *Hand1* expression. Consistent with this, left-sided expression in the anterior portion of the heart tube is transitory, being replaced by ventrally restricted expression even before the onset of looping (data not shown).

In the mouse, a similarly complex pattern of *Hand1* expression has been described in the linear heart tube (Biben and Harvey, 1997; Thomas *et al.*, 1998). The caudal domain of expression in the mouse heart is initially restricted to the ventral side of the linear heart tube but expression becomes enhanced on the left side of more cranial region. This sidedness is maintained through the onset of looping, with the result that Hand1 transcripts are localised to the outer curvature of the future left ventricle. Overall, the resulting pattern of an asymmetric, left-sided distribution in the anterior/cranial portion of the heart tube becoming ventral and more symmetrical in the posterior/caudal region is similar in both frog and mouse embryos prior to looping.

Subsequent differences between the mouse data and our results may not be as profound as they appear, if account is taken of the differing topologies of heart looping. The accentuated spiral nature of looping in the *Xenopus* embryo could have the result that the initial right–left axis of the heart tube becomes shifted towards the dorsoventral axis of the embryo. Because of this, the ventral region of the myocardium within the central portion of the looped tube probably forms the outer curvature of the presumptive ventricle. A similar relationship has previously been demonstrated by cell-labelling experiments in the chick embryo (de la Cruz *et al.*, 1997). This part of the myocardial wall subsequently expands due the formation of trabeculae (Moorman and Lamer, 1998, and Fig. 7G).

In the mouse, Hand1 expression is largely restricted to the left (systemic) ventricle whilst that of the other Hand gene, Hand2, is enhanced in the right (pulmonary) ventricle. Our finding that *Xenopus* Hand1 expression extends throughout the prospective ventricular region could be interpreted in two ways. Either the chamber-restricted pattern of Hand1 expression is not conserved between mouse and frog or the single *Xenopus* ventricle corresponds to the left ventricle of mammals. In either case, our findings point to important evolutionary differences in the early patterning of the heart tube amongst vertebrates. Further investigation of these possibilities awaits identification of other early regional heart markers and characterisation of *Xenopus Hand2* expression.

ACKNOWLEDGMENTS

We thank Wendy Hatton and Ian Harragon (NIMR Histology Service) for expert technical assistance, Masazumi Tada (NIMR) for whole-mount immunostaining of the tadpole notochord, and John McLachlan (University of St. Andrews) for helpful discussions of 3D reconstruction techniques. This work was supported by the British Heart Foundation.

REFERENCES

Amaya, E., Offield, M. F., and Grainger, R. M. (1998). Frog genetics: Xenopus tropicalis jumps into the future. *Trends Genet.* **14,** 253–255.

Biben, C., and Harvey, R. P. (1997). Homeodomain factor Nkx2-5 controls left/right asymmetric expression of bHLH gene eHand during murine heart development. *Genes Dev.* **11,** 1357–1369.

Chambers, A. E., Logan, M., Kotecha, S., Towers, N., Sparrow, D., and Mohun, T. J. (1994). The RSRF/MEF2 protein SL1 regulates cardiac muscle-specific transcription of a myosin light-chain gene in Xenopus embryos. *Genes Dev.* **8,** 1324–1334.

Cleaver, O. B., Patterson, K. D., and Krieg, P. A. (1996). Overexpression of the tinman-related genes XNkx-2.5 and XNkx-2.3 in Xenopus embryos results in myocardial hyperplasia. *Development* **122,** 3549–3556.

Copenhaver, W. M. (1926). Experiments on the development of the heart of *Ambystoma punctatum*. *J. Exp. Zool.* **43,** 321–371.

de la Cruz, M. V., Castillo, M. M., Villavicencio, L., Valencia, A., and Moreno-Rodriguez, R. A. (1997). Primitive interventricular septum, its primordium, and its contribution in the definitive interventricular septum: In vivo labelling study in the chick embryo heart. *Anat. Rec.* **247,** 512–520.

Drysdale, T. A., Tonissen, K. F., Patterson, K. D., Crawford, M. J., and Krieg, P. A. (1994). Cardiac troponin I is a heart-specific marker in the *Xenopus* embryo: Expression during abnormal heart morphogenesis. *Dev. Biol.* **165,** 432–441.

Evans, S. M., Yan, W., Murillo, M. P., Ponce, J., and Papalopulu, N. (1995). tinman, a Drosophila homeobox gene required for heart and visceral mesoderm specification, may be represented by a family of genes in vertebrates: XNkx-2.3, a second vertebrate homologue of tinman. *Development* **121,** 3889–3899.

Firulli, A. B., McFadden, D. G., Lin, Q., Srivastava, D., and Olson, E. N. (1998). Heart and extra-embryonic mesodermal defects in mouse embryos lacking the bHLH transcription factor Hand1. *Nat. Genet.* **18,** 266–270.

Fishman, M. C., and Chien, K. R. (1997). Fashioning the vertebrate heart: Earliest embryonic decisions. *Development* **124,** 2099–2117.

Fu, Y., Yan, W., Mohun, T. J., and Evans, S. M. (1998). Vertebrate tinman homologues XNkx2-3 and XNkx2-5 are required for heart formation in a functionally redundant manner. *Development* **125,** 4439–4449.

Horb, M. E., and Thomsen, G. H. (1999). Tbx5 is essential for heart development. *Development* **126,** 1739–1751.

Kelly, R. G., Zammit, P. S., and Buckingham, M. E. (1999). Cardiosensor mice and transcriptional subdomains of the vertebrate heart. *Trends Cardiovasc. Med.* **9,** 3–10.

Kolker, S., Tajchman, U., and Weeks, D. L. (1999). Confocal imaging of early heart development in *Xenopus laevis*. Submitted for publication.

Kroll, K. L., and Amaya, E. (1996). Transgenic Xenopus embryos from sperm nuclear transplantations reveal FGF signaling requirements during gastrulation. *Development* **122,** 3173–3183.

Lin, Q., Schwarz, J., Bucana, C., and Olson, E. N. (1997). Control of mouse cardiac morphogenesis and myogenesis by transcription factor MEF2C. *Science* **276,** 1404–1407.

Logan, M., and Mohun, T. (1993). Induction of cardiac muscle differentiation in isolated animal pole explants of Xenopus laevis embryos. *Development* **118,** 865–875.

Lyons, I., Parsons, L. M., Hartley, L., Li, R., Andrews, J. E., Robb, L., and Harvey, R. P. (1995). Myogenic and morphogenetic defects in

the heart tubes of murine embryos lacking the homeo box gene Nkx2-5. *Genes Dev.* **9,** 1654–1666.

Millard, N. (1945). The development of the arterial system of *Xenopus laevis,* including experiments on the destruction of the larval aortic arches. *Trans. R. Soc. S. Afr.* **30,** 217–234.

Millard, N. (1949). The development of the venous system of *Xenopus laevis. Trans. R. Soc. S. Afr.* **32,** 55–99.

Mohun, T. J., and Leong, L. M. (1998). Heart formation and the heart field in amphibian embryos. *In* "Heart Development" (R. P. Harvey and N. Rosenthal, Eds.), pp. 37–49. Academic Press, San Diego.

Moorman, A. F. M., and Lamer, W. H. (1998). Development of the conduction system of the vertebrate heart. *In* "Heart Development" (R. P. Harvey and N. Rosenthal, Eds.), pp. 195–208. Academic Press, San Diego.

Nieuwkoop, P., and Faber, J. (1956). "Normal Table of *Xenopus laevis* (Daudin)." North-Holland, Amsterdam.

Raffin, M., Leong, L. M., Rones, M. S., Sparrow, D. B., Mohun, T., and Mercola, M. (1999). Subdivision of the cardiac Nkx2.5 expression domain into myogenic and non-myogenic compartments. *Dev. Biol.* in press.

Riley, P., Anson-Cartwright, L., and Cross, J. C. (1998). The Hand1 bHLH transcription factor is essential for placentation and cardiac morphogenesis. *Nat. Genet.* **18,** 271–275.

Sater, A. K., and Jacobson, A. G. (1990). The restriction of the heart morphogenetic field in *Xenopus laevis. Dev. Biol.* **140,** 328–336.

Sparrow, D. B., Kotecha, S., Towers, N., and Mohun, T. J. (1998). Xenopus eHAND: A marker for the developing cardiovascular system of the embryo that is regulated by bone morphogenetic proteins. *Mech. Dev.* **71,** 151–163.

Srivastava, D., Cserjesi, P., and Olson, E. N. (1995). A subclass of bHLH proteins required for cardiac morphogenesis. *Science* **270,** 1995–1999.

Srivastava, D., Thomas, T., Lin, Q., Kirby, M. L., Brown, D., and Olson, E. N. (1997). Regulation of cardiac mesodermal and neural crest development by the bHLH transcription factor, dHAND. *Nat. Genet.* **16,** 154–160.

Streicher, J., Weninger, W. J., and Muller, G. B. (1997). External marker-based automatic congruencing: A new method of 3D reconstruction from serial sections. *Anat. Rec.* **248,** 583–602.

Thomas, T., Yamagishi, H., Overbeek, P. A., Olson, E. N., and Srivastava, D. (1998). The bHLH factors, dHAND and eHAND, specify pulmonary and systemic cardiac ventricles independent of left–right sidedness. *Dev. Biol.* **196,** 228–236.

Tonissen, K. F., Drysdale, T. A., Lints, T. J., Harvey, R. P., and Krieg, P. A. (1994). XNkx-2.5, a *Xenopus* gene related to Nkx-2.5 and tinman: Evidence for a conserved role in cardiac development. *Dev. Biol.* **162,** 325–328.

Weninger, W. J., Meng, S., Streicher, J., and Muller, G. B. (1998). A new episcopic method for rapid 3-D reconstruction: Applications in anatomy and embryology. *Anat. Embryol. (Berlin)* **197,** 341–348.

Received for publication September 7, 1999
Revised October 27, 1999
Accepted November 1, 1999